In vivo and *in vitro* oncogenic effects of *HIF2A* mutations in pheochromocytomas and paragangliomas

Rodrigo A Toledo[1,*], Yuejuan Qin[1,*], Subramanya Srikantan[1], Nicole Paes Morales[1], Qun Li[1], Yilun Deng[1], Sang-Woo Kim[1,†], Maria Adelaide A Pereira[3], Sergio P A Toledo[3], Xiaoping Su[4], Ricardo C T Aguiar[1,2] and Patricia L M Dahia[1,2]

[1]Division of Hematology and Medical Oncology, Department of Medicine, Cancer Therapy and Research Center at the University of Texas Health Science Center, 7703 Floyd Curl Drive, MC 7880, San Antonio, Texas 78229-3900, USA
[2]Greehey Children Cancer Research Institute, San Antonio, Texas, USA
[3]University of São Paulo School of Medicine, São Paulo, SP, Brazil
[4]Department of Bioinformatics and Computational Biology, The University of Texas MD Anderson Cancer Center, Houston, Texas, USA
*(R A Toledo and Y Qin contributed equally to this work)
[†]S-W Kim is now at Department of Biological Sciences, College of Natural Sciences, Pusan National University, Busan 609-735, Republic of Korea

Correspondence should be addressed to P L M Dahia
Email
dahia@uthscsa.edu

Abstract

Pheochromocytomas and paragangliomas are highly vascular tumors of the autonomic nervous system. Germline mutations, including those in hypoxia-related genes, occur in one third of the cases, but somatic mutations are infrequent in these tumors. Using exome sequencing of six paired constitutive and tumor DNA from sporadic pheochromocytomas and paragangliomas, we identified a somatic mutation in the *HIF2A* (*EPAS1*) gene. Screening of an additional 239 pheochromocytomas/paragangliomas uncovered three other *HIF2A* variants in sporadic (4/167, 2.3%) but not in hereditary tumors or controls. Three of the mutations involved proline 531, one of the two residues that controls HIF2α stability by hydroxylation. The fourth mutation, on Ser71, was adjacent to the DNA binding domain. No mutations were detected in the homologous regions of the *HIF1A* gene in 132 tumors. Mutant *HIF2A* tumors had increased expression of *HIF2*α target genes, suggesting an activating effect of the mutations. Ectopically expressed *HIF2*α mutants in HEK293, renal cell carcinoma 786-0, or rat pheochromocytoma PC12 cell lines showed increased stability, resistance to VHL-mediated degradation, target induction, and reduced chromaffin cell differentiation. Furthermore, mice injected with cells expressing mutant *HIF2A* developed tumors, and those with Pro531Thr and Pro531Ser mutations had shorter latency than tumors from mice with wild-type *HIF2A*. Our results support a direct oncogenic role for *HIF2A* in human neoplasia and strengthen the link between hypoxic pathways and pheochromocytomas and paragangliomas.

Key Words
- pheochromocytoma
- paraganglioma
- hypoxia
- cancer
- mutations
- HIF2A
- EPAS1
- somatic

Endocrine-Related Cancer (2013) **20**, 349–359

Endocrine-Related Cancer

http://erc.endocrinology-journals.org
DOI: 10.1530/ERC-13-0101

Published by Bioscientifica Ltd.

Introduction

Pheochromocytomas and paragangliomas are sympathetic neural-derived neoplasms. Over one third of these tumors carry germline mutations in one of the ten distinct genes (Jafri & Maher 2012). Remarkably, somatic events in pheochromocytomas have been limited to mutations of some of these susceptibility genes (Burnichon *et al*. 2011).

A majority of hereditary pheochromocytomas and paragangliomas are related to the hypoxia pathway through mutations of the *VHL* gene or those encoding the succinate dehydrogenase (SDH) complex (Jafri & Maher 2012). Loss-of-function mutations in these genes lead to increased stability of main components of the response to low oxygen levels, the hypoxia-inducible factor (HIF) proteins (Gimenez-Roqueplo *et al*. 2001, Dahia *et al*. 2005). The HIF transcription factors form heterodimers comprised of an inducible, oxygen-labile α-subunit (HIF1α, HIF2α, or HIF3α) and a stable β-subunit (HIF1β/ARNT) that bind to the promoter of multiple genes associated with angiogenesis, glycolysis, and cell growth. Stability of HIFα subunits is dependent on their hydroxylation at two specific prolines by oxygen-dependent prolyl hydroylases (PHDs; Kaelin & Ratcliffe 2008). Hydroxylation of HIFα subunits at these two prolyl residues (Pro405 and Pro531 in HIF2α), located at the oxygen-dependent degradation domain (ODD), make it recognizable by VHL for binding and subsequent proteasome-mediated degradation. The activity of PHDs is regulated in part by the abundance of the SDH substrate, succinate, which accumulates when SDH is deficient (Selak *et al*. 2005). As a result, mutations in *VHL* or *SDH* (*SDHB*) genes confer a distinctive pseudohypoxic profile to pheochromocytomas and paragangliomas (Dahia *et al*. 2005, Burnichon *et al*. 2011).

Deregulation of HIFα, specifically HIF2α, has long been implicated in tumorigenesis and in poor prognosis of various human cancers (Qing & Simon 2009). In particular, HIF2α activation was shown to be both necessary and sufficient for the development of VHL-null renal cell carcinomas (Kondo *et al*. 2002, 2003). In addition, other stimuli can lead to increased HIF2α activity in many malignancies (Qing & Simon 2009). However, HIF2α has also been proposed to function as a tumor suppressor in lung adenocarcinoma and gliomas (Acker *et al*. 2005, Mazumdar *et al*. 2010). Furthermore, germline *HIF2A* mutations confer susceptibility to familial erythrocytosis, a disorder not typically associated with tumors (Percy *et al*. 2006). The absence of direct genetic evidence of *HIF2A* oncogenicity has contributed to fuel the controversy over its role in cancers. Here, we report mutations of the *HIF2A* gene in pheochromocytomas identified by exome sequencing. Our findings extend recent candidate gene-based observations of *HIF2A* mutations in these tumors (Favier *et al*. 2012, Lorenzo *et al*. 2012, Zhuang *et al*. 2012, Comino-Mendez *et al*. 2013, Pacak *et al*. 2013) by showing that these variants confer growth advantage *in vivo*, supporting their role as driver events in the pathogenesis of pheochromocytomas and paragangliomas.

Materials and methods

Patients and samples

Tumor and matching normal tissue were obtained from patients with pheochromocytomas and paragangliomas according to institutionally approved protocols. Details on this cohort of 239 tumors are provided in Supplementary Materials and methods, see section on supplementary data given at the end of this article. Normal tissue was obtained from blood or adjacent normal tissue.

DNA and RNA isolation

Blood and tumor DNA and RNA were isolated using Qiagen kits or Trizol respectively following the manufacturers' protocols.

Exome sequencing

We performed whole exome sequencing of matched germline and tumor DNA from six pheochromocytomas/paragangliomas without an identifiable *PSG* (*PSG5*) mutation. Libraries were prepared and exomes enriched using Agilent Sure Select 44Mbp at the Beijing Genomics Institute, as described (Gui *et al*. 2011). Paired-end reads of enriched exomes were generated in Illumina HiSeq2000 (average depth of 50×) and aligned using the Mosaik algorithm (Hillier *et al*. 2008). Variants detected at the somatic level were selected using a modified version of the GigaBayes/FreeBayes pipeline for somatic variants (Marth *et al*. 1999). Synonymous sequence variants and those present in the dbSNP135 database were excluded.

Sanger sequencing

Primers flanking the 16 exons of the *HIF2A* gene and exons 9, 12, and 16 of *HIF1A* (sites of three regulatory hydroxylation domains) were used for PCRs and

http://erc.endocrinology-journals.org
DOI: 10.1530/ERC-13-0101

Published by Bioscientifica Ltd.

Sanger sequencing as described in Supplementary Materials and methods.

Microarray-based expression profiling

We used normalized transcription data from 126 pheochromocytomas that were generated using Affymetrix U133 microarrays (GEO accession numbers GSE28416 and GSE199877) (Dahia *et al.* 2005, Qin *et al.* 2010). Two *HIF2A* mutant tumors (37 and 208) were available in this cohort and were used for comparisons with tumors from other well-established hereditary pheochromocytomas. Details are described in Supplementary Materials and methods.

Quantitative Real-time PCR (qRT-PCR)

This was performed in cDNA isolated from tumors and cell lines (Qin *et al.* 2010). Additional details are provided in Supplementary Materials and methods.

Clones and constructs

A HA-HIF2alpha-pBabe-puro construct containing the wild-type HIF2A coding sequence, originated from Dr Willam Kaelin's laboratory (Kondo *et al.* 2003), was obtained from Addgene, Cambridge, MA, USA. Site-direct mutagenesis was used to generate each of the *HIF2A* mutants as described, all maintaining the wild-type Pro405, to mimic the tumor-related mutations (Qin *et al.* 2010). An HA-tagged full-length VHL construct was cloned into the MSCV-GFP retroviral vector.

Cell culture, transductions, and transfections

HEK293, 786-0, and PC12 cell lines were cultured as described in Supplementary Materials and methods. For hypoxia experiments, cells were maintained in a hypoxia chamber at 1% O_2 (InVivo200, Ruskinn, Bridgend, UK) for 16 h. Retroviral transduction was performed as described (Qin *et al.* 2010). MSCV-HA-VHL constructs were sorted by flow cytometry based on GFP expression (Qin *et al.* 2010). Puromycin-resistant pools or clones were obtained.

Cycloheximide assay

HEK293 cells stably expressing wild-type or various *HIF2A* mutants were treated with cycloheximide 100 μg/ml for the indicated times.

Nerve growth factor differentiation and withdrawal

PC12 cells were exposed to nerve growth factor (NGF) 50 ng/ml (Harlan, Houston, TX, USA) for 5–7 days followed by its withdrawal for 24 h, as described previously (Lee *et al.* 2005).

Nude mouse xenografts

Nude mouse xenograft assays were performed as described (Rai *et al.* 2010). Cells stably expressing empty vector, wild-type HIF2α, and 531 mutants were injected subcutaneously in nude mice (six or seven mice per group). Animals were killed after 28 days and tumor weights were recorded. Two additional cohorts were performed and in these, animals that developed tumors ($n=5$–10 per group) were killed when tumor reached maximum size, following UTHSCSA-IACUC-approved protocols.

Statistical analysis

The statistical significance of *in vitro* assays was determined with a two-tailed Student's *t*-test and one-way ANOVA or Kruskal–Wallis for the xenograft assay. In all instances, $P<0.05$ was considered significant. Data analyses were performed with the Prism software (GraphPad, La Jolla, CA, USA) and Excel (Microsoft).

Results

Sporadic pheochromocytomas and paragangliomas carry somatic mutations of the *HIF2A* but not *HIF1A* gene

To discover novel somatic mutations involved in pheochromocytomas and paragangliomas, we generated exome sequences of six paired constitutive and tumor DNA samples without a mutation in any of the known pheochromocytoma susceptibility genes. We identified 269 somatic variants and herein focus on a heterozygous *HIF2A* gene mutation affecting the hydroxyl-acceptor residue, proline 531 (Pro531Thr), identified in one of these patients (Table 1).

This mutation was confirmed by Sanger sequencing in the tumor and was absent from the patient's germline DNA (Fig. 1A). We next extended the screening of the entire *HIF2A* coding sequence to 239 pheochromocytomas/paragangliomas, including 166 sporadic and 72 with a germline PSG mutation. We identified 32 variants (Supplementary Table 1, see section on supplementary data given at the end of this article), of which four, including the change originally detected in the exome,

http://erc.endocrinology-journals.org
DOI: 10.1530/ERC-13-0101

Published by Bioscientifica Ltd.

Table 1 Summary of mutant cases clinical and genetic features.

Sample ID	Age	Gender	Tumor location	Malignancy status	Other disease	Familial	Sequence variant (nucleotide)	Sequence variant (protein)	Heterozygosity at the mutation site	Polyphen2/SIFT[a] prediction
9	10	M	Periadrenal	Lymph node metastases	No	N	c.1591C>AC[b]	p.Pro531Thr	Y	Damaging
208	47	F	Periaortic	Unknown	No	N	c.1591C>TC	p.Pro531Ser	Y	Damaging
37	72	F	Adrenal	Unknown	No	N	c.1592C>TC	p.Pro531Leu	Y	Damaging
100 288[c]	?	F	Adrenal	Unknown	?	?	c.212C>AC	p. Ser71Tyr	Y	Damaging

[a]PolyPhen and Sift are softwares that predict the possible impact of an amino acid substitution on the structure and function of a protein.
[b]Variant found by exome sequencing, confirmed by Sanger sequence.
[c]Sample obtained from tumor bank, limited data available.

fulfilled our criteria for pathogenic significance: involved a conserved residue, were absent in controls, and were predicted to change protein function *in silico* (Table 1). Similar to the exome finding, two other variants also targeted the 531 codon (Pro531Ser and Pro531Leu). The remaining one was detected immediately distal to the DNA binding domain of HIF2α (Ser71Tyr). All the four variants were found in sporadic, but not hereditary, pheochromocytomas and paragangliomas (four of 167 tumors, 2.3%) and were absent in an ethnically matched control group ($n=214$ alleles) or publicly available sequences from the SNP database (http://www.ncbi.nlm.nih.gov/snp/) and 1000 Genomes Project (http://www.1000genomes.org/). The mutations were exclusively detected in tumor DNA of two cases in which germline material was available (Fig. 1A). In two other samples, the somatic status of the mutations could be established due to unavailability of constitutive DNA. The homologous region of the *HIF1A* gene was also sequenced in 132 of these tumors, including the tumors with *HIF2A* mutations, but no pathogenic variants were identified (Supplementary Table 1).

Clinically, two of the mutations occurred in paragangliomas, one metastatic and the other recurrent, while the other two were in pheochromocytomas (Table 1). All four tumor DNA sequence traces had a heterozygous appearance, indicating retention of both alleles (Fig. 1A). In one case, sequence of tumor cDNA showed that both alleles were transcribed (Supplementary Figure 1).

HIF2A mutations induce target genes in primary tumors and cell lines and increase HIF2α stability

The clustering of the mutations (3/4) at the primary site of HIF2α hydroxylation suggested that these variants are functionally relevant (Fig. 1B). To explore the consequences of these *HIF2A* mutations, we measured expression of HIF target genes in primary tumor samples. Two of the tumors, carrying a mutation on Pro531Ser and Pro531Leu, had been previously included in our global transcriptional study of pheochromocytomas (Dahia *et al.* 2005). Reassuringly, both *HIF2A* mutant tumors aligned with the pseudohypoxic group, which was comprised of samples carrying germline *VHL* and *SDHB* or *SDHD* gene mutations (known as cluster 1), by supervised clustering analysis (Dahia *et al.* 2005). Normalized data from probes encoding HIF target genes were extracted from this dataset and plotted against expression data from other pheochromocytomas carrying either cluster 1 or cluster 2 (*RET*, *NF1*, or *TMEM127*) mutations (Fig. 1C). RNA was also obtained

http://erc.endocrinology-journals.org
DOI: 10.1530/ERC-13-0101

Published by Bioscientifica Ltd.

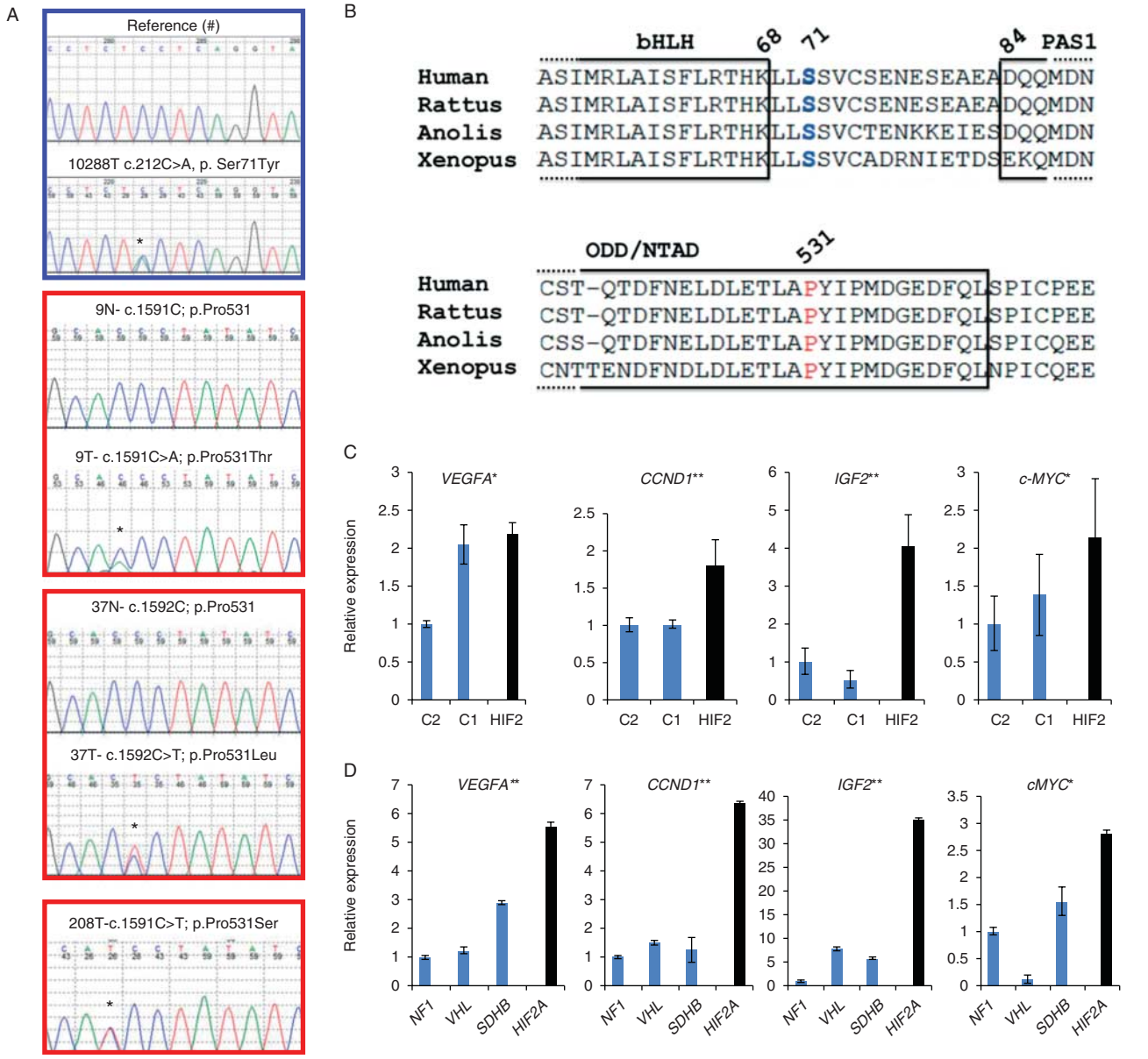

Figure 1

Somatic mutations of *HIF2A* in pheochromocytomas and paragangliomas. (A) Sequence traces of tumor DNA showing the four mutations identified (Ser71Tyr, Pro531Thr, Pro531Leu, and Pro531Ser) and either their respective normal sequences from germline DNA or a reference control (#). Mutations are indicated with an asterisk. Border coloring matches the mutated amino acid on HIF2α sequence shown in B. (B) Amino acid sequence alignment of HIF2α showing high conservation at the DNA binding domain (basic helix–loop–helix = bHLH), PAS1 (PER-ARNT-SIM) domain, and the N-terminal transactivation domain (N-TAD) oxygen-dependent degradation domain (ODD) across various species. The residues mutated in pheochromocytomas and paragangliomas are shown in color, matching the respective DNA sequences displayed in (A). (C) Expression levels of *VEGFA*, *CCND1*, *IGF2*, and *c-MYC* transcripts obtained from microarray-based profiling of combined *HIF2A* mutant tumors (37 and 208 = HIF2) in comparison with pheochromocytomas mutated for *NF1* and *TMEM17* genes (C2 = cluster 2) and *VHL*, *SDHB*, and *SDHD* genes (C1 = cluster 1), as detailed in the Materials and methods section. Values of the C2 cluster samples have been set to 1 (*statistically significant difference between *HIF2A* mutant and C2 tumors; **statistically significant difference between *HIF2A* mutant samples and both C1 and C2 tumors, at $P<0.05$).
(D) Expression levels of *VEGFA*, *CCND1*, *IGF2*, and *c-MYC* transcripts in one *HIF2A*-mutated primary tumor (tumor from sample 9) along with other pheochromocytomas carrying mutations of *VHL*, *SDHB*, or *NF1* genes assayed by quantitative real-time PCR (qRT-PCR). Samples were run in triplicate and the experiment was repeated at least twice. Results are shown as the average and bars represent S.E.M. Values of NF1 samples were set to 1. (*statistically significant difference between *HIF2A* mutant samples and NF1 tumors, **statistically significant difference between *HIF2A* mutant samples and *NF1*-, *VHL*- or *SDHB*-related tumors, at $P<0.05$).

http://erc.endocrinology-journals.org
DOI: 10.1530/ERC-13-0101

Published by Bioscientifica Ltd.

from another *HIF2A* mutant tumor and compared to genetically defined pheochromocytomas or paragangliomas. Quantitative real-time PCR (qRT-PCR) of HIF-responsive genes encoding *VEGFA*, cyclin D1 (*CCND1*), *IGF2*, and *c-MYC* (*MYC*) was performed in these tumors (Fig. 1D). The *HIF2A* mutant tumors, both by microarray and by qRT-PCR analyses, displayed increased target gene expression (Fig. 1C and D). Moreover, cyclin D1 (also known as CCND1) and c-MYC, considered HIF2α-specific growth-promoting determinants in renal cell carcinomas (Raval *et al*. 2005, Gordan *et al*. 2007), and IGF2, associated with hypoxic neuroblastomas (Pietras *et al*. 2009), were also induced, suggesting that these effectors may contribute to the protumorigenic effects of *HIF2A* mutations in pheochromocytomas/paragangliomas.

The site of the mutations on the critical 531 prolyl residue suggested that these variants affected *HIF2A* stability. We examined these effects by generating HEK293 cell lines stably expressing each mutation, created by site-directed mutagenesis in a retroviral backbone. Constructs containing wild-type 531 sequence or a *HIF2A* mutation (Pro531Ala), previously shown to be both resistant to PHD action and defective in VHL binding (Kondo *et al*. 2002), were also used. All constructs, analogous to the primary tumors, were wild type for proline 405, the secondary HIF2α hydroxylation site. Stable expression of the *HIF2A* 531 mutations led to increased stability and prolonged half-life of *HIF2A in vitro* under normoxia to levels similar to those seen with the Pro531Ala mutant, as shown by a time course assay with cycloheximide (Fig. 2A and Supplementary Figure 2, see section on supplementary data given at the end of this article). These findings are consistent with structural studies of HIF1α indicating that replacement of the equivalent proline (Pro564) with other residues prevents hydroxylation at this site (Min *et al*. 2002). The expression levels of the juxta-DNA binding domain mutation, Ser71Tyr, in contrast, did not differ from the levels of the wild-type construct, suggesting that this mutation does not affect HIF2α stability (Fig. 2A).

Mutant *HIF2α* is stabilized by hypoxia and is resistant to VHL-mediated degradation

Despite already high normoxic levels of mutant *HIF2A* in HEK293 cells, these constructs could be further stabilized and activated by hypoxia, as measured by an increase in HA-HIF2A and GLUT1 protein abundance respectively (Fig. 2B). This response likely results from the effect of hypoxia on the intact proline 405, which leads to HA-HIF2A product escape from VHL-mediated proteasome degradation. Similar to the primary tumors, HEK293 cell lines expressing *HIF2A* mutations showed increased expression of *VEGFA*, *OCT4/POU5F1*, and *GLUT1/SLC2A1* transcripts (Fig. 2C). These results suggest that the 531 mutations are associated with constitutive HIF2α activation.

We next stably expressed the *HIF2A* mutants in the VHL-null 786-0 renal carcinoma cells reconstituted with VHL and measured transcription of target genes. Again, mutants showed increased expression of *VEGFA*, *OCT4/POU5F1*, and *GLUT1/SLC2A1* (Fig. 2D). We also compared GLUT1 protein levels in 786-0 cells expressing various *HIF2A* mutations without VHL or after its reconstitution. VHL expression normalized GLUT1 in cells expressing endogenous HIF2α and an empty vector control, as expected, but it was unable to overcome the effect of the new mutations or the positive control HIF2A Pro531Ala on this target (Fig. 2E). These results suggest that mutations of this site abrogate VHL binding to the HIF2α ODD (Kondo *et al*. 2002). Unlike the 531 mutants, HIF2A-Ser71Tyr mutant expression was undetectable in the presence of VHL similar to wild-type HIF2A (Supplementary Figure 3, see section on supplementary data given at the end of this article), suggesting that binding to VHL was not altered by this variant.

HIF2A mutations change the differentiation pattern of chromaffin cells

To explore the effect of *HIF2A* mutations in a more tissue-specific context, we used rat pheochromocytoma PC12 cells. Expression of the four *HIF2A* mutants also led to increased target transcription in comparison with empty vector-expressing cells (Fig. 3A). PC12 cells are capable of differentiating into neurons after exposure to NGF (Lee *et al*. 2005). Under these conditions, cells extended neurites and increased expression of chromaffin cell markers chromogranin A (CHGA) and neuropeptide Y (NPY), while transcription of HIF2A, its target, VEGFA, and a marker of cell dedifferentiation, *Nanog*, were decreased (Supplementary Figure 4A, see section on supplementary data given at the end of this article). In contrast, exposure of PC12 cells expressing various *HIF2A* mutations to NGF for 7 days led to reduced transcription of *CHGA* and *NPY* in comparison with cells expressing empty vector (Fig. 3B). Likewise, chromaffin markers NPY and dHAND were downregulated in a *HIF2A* mutant tumor (Fig. 3C), suggesting that the PC12 model recapitulates *in vivo* effects of these mutations. Furthermore, markers of cell dedifferentiation or stemness, *NANOG*, *OCT4*, *JAGGED2*

http://erc.endocrinology-journals.org
DOI: 10.1530/ERC-13-0101

Published by Bioscientifica Ltd.

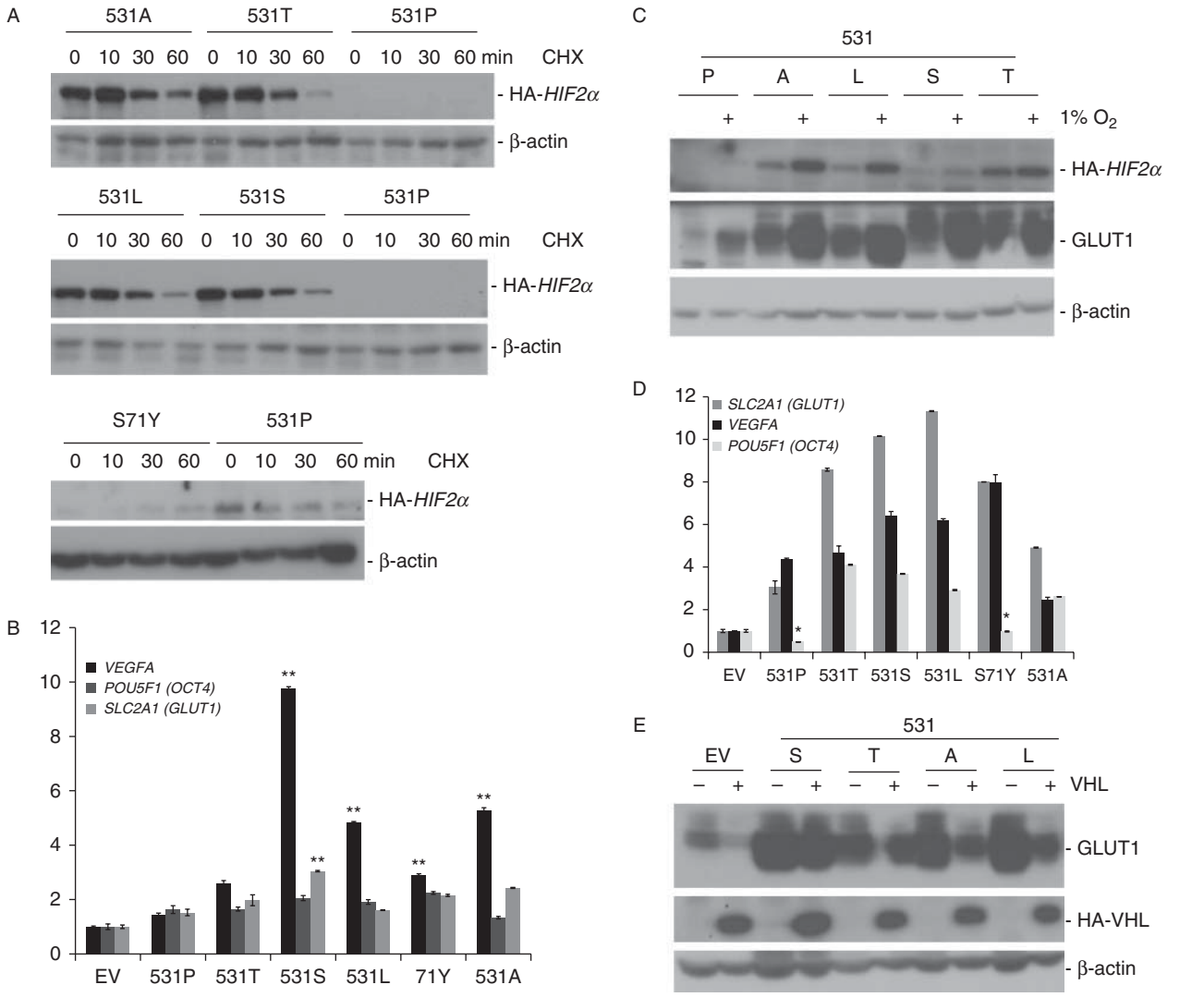

Figure 2

HIF2A mutations lead to prolonged stability of the protein, activation of downstream targets, and resistance to VHL-mediated degradation *in vitro*. (A) HEK293 cell lines were retrovirally infected to stably produce HA-tagged wild-type or various *HIF2A* mutants (Pro531Thr=531T, Pro531Leu=531L, Pro531Ser=531S, and Ser71Tyr=S71Y) or wild-type (531P) as indicated. The Pro531Ala (P531A) mutant construct is included as a positive control (Kondo *et al*. 2002). Cell extracts were prepared after cycloheximide exposure for the indicated times and immunoblotted with anti-HA antibody or β-actin as a loading control. (B) Transcript levels of *VEGFA*, *POU5F1* (*OCT4*), and *SLC2A1* (*GLUT1*) of HEK293 cells stably expressing the indicated *HIF2A* mutants and controls, measured by quantitative real-time PCR (qRT-PCR). Results are shown as the average and bars represent S.E.M. Values were normalized to those of EV control (*statistical significance at $P<0.05$; **statistical significance at $P<0.005$ between cells expressing each HIF2A construct vs EV). (C) HEK293 cells expressing *HIF2A* mutants or wild-type control were incubated overnight under normoxia or 1% O_2, as shown. Cell extracts were prepared and probed with anti-HA, anti-GLUT1, or a loading control, β-actin. (D) Transcript levels of *VEGFA*, *POU5F1* (*OCT4*), and *SLC2A1* (*GLUT1*) in VHL-reconstituted 786-0 cells stably expressing the indicated *HIF2A* mutants and controls, measured by qRT-PCR. Results were normalized to those of EV control (*non-significance; all remaining values showed statistical significance at $P<0.005$ between cells expressing each HIF2A construct vs EV). (E) 786-0 renal carcinoma cells stably expressing the designated 531 *HIF2A* mutants were reconstituted with an MSCV-HA-VHL retroviral construct or control. Cell extracts were prepared and immunoblotted with GLUT1, HA, and β-actin was a loading control.

(*JAG2*), *KRT19*, *SOX9*, and *CHD2*, were increased in *HIF2A* mutant pheochromocytomas/paragangliomas (Fig. 3C and D). This differential transcription pattern is reminiscent of the effects of hypoxia, and specifically, HIF2α, in promoting an immature, stem cell-like phenotype of the sympathetic-derived tumors neuroblastomas (Pietras *et al*. 2009). Thus, increased HIF2α activation caused by these mutations may lead to a shift in the NGF-induced transcriptional program. Parenthetically, we did not detect differences in apoptosis of these cells following

http://erc.endocrinology-journals.org
DOI: 10.1530/ERC-13-0101

Published by Bioscientifica Ltd.

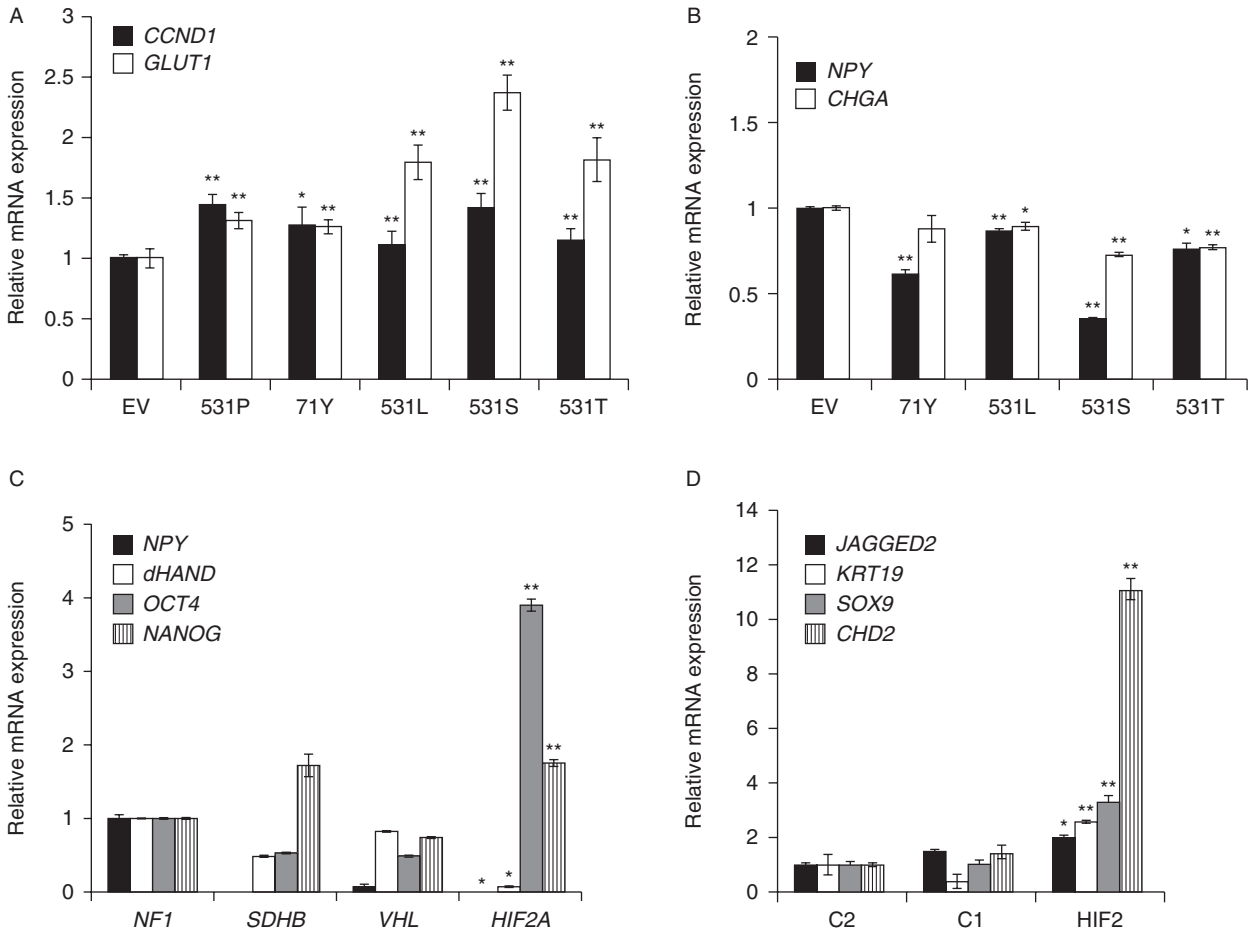

Figure 3

HIF2A mutations activate downstream targets and reduce expression of nerve growth factor (NGF)-induced chromaffin differentiation markers in pheochromocytoma cells. (A) Expression levels of *CCND1* and GLUT1 (*SLC2A1*) transcripts of undifferentiated PC12 cells stably expressing an empty vector (EV), the indicated *HIF2A* mutants (Ser71Tyr=71Y, Pro531Thr=T, Pro531Leu=L, and Pro531Ser=S), or a wild-type (P) HIF2A construct by quantitative real-time PCR (qRT-PCR). Samples were run in triplicate and experiment was repeated twice. Results are shown as the average and bars represent S.E.M. Values of EV-expressing cells were set to 1 (*statistical significance between each *HIF2A* mutant and empty vector at $P<0.05$; **statistical significance between each *HIF2A* mutant and an empty vector at $P<0.001$). (B) Expression levels of *NPY* and *CHGA* transcripts by qRT-PCR of PC12 cells stably expressing the designated *HIF2A* constructs or an empty vector (EV) after 7 days of exposure to 50 ng/ml NGF (*$P<0.001$ EV vs all mutants, **$P<0.0001$ EV vs all mutants), performed as in (A). (C) Expression of *NPY*, *dHAND* (*HAND2*), *OCT4*, and *NANOG* transcripts in *HIF2A*-mutated paraganglioma from sample 9 along with other pheochromocytomas carrying mutations of *VHL*, *SDHB*, or *NF1* genes. Samples were run in triplicate. Results are shown as the average and bars represent S.E.M. Values of NF1 samples were set to 1. All results were statistically significant between the *HIF2A* mutant tumor and NF1 at *$P<0.01$ or **$P<0.001$). (D) Expression of stemness-related genes *JAGGED2*, *KRT19*, *SOX9*, and *CHD2* in transcripts obtained from microarray-based profiling of combined *HIF2A* mutant tumors (37 and 208=HIF2) in comparison with pheochromocytomas mutated for *NF1* and *TMEM17* genes (C2=cluster 2) and *VHL*, *SDHB*, and *SDHD* genes (C1=cluster 1), as detailed in the Materials and methods section. Values of the C2 cluster samples have been set to 1 (*statistically significant difference between *HIF2A* mutant and C2 tumors; **statistically significant difference between *HIF2A* mutant samples and both C1 and C2 tumors, at $P<0.05$).

NGF removal (Supplementary Figure 4B), in agreement with earlier findings of a HIF-independent, inhibitory effect of pheochromocytoma mutations in sympathetic precursor cell death (Lee *et al.* 2005). The downregulation of chromaffin markers in both mutant *HIF2A* cell lines and tumors accompanied by the increased expression of dedifferentiation markers are consistent with the notion that mutant *HIF2α* may contribute to a less differentiated phenotype of pheochromocytomas and paragangliomas.

HIF2A mutations promote tumor growth in mice

No changes were seen in *HIF2A* mutant cell proliferation *in vitro*, similar to reports of *HIF2A* overexpression in renal carcinomas (Supplementary Figure 5, see section on

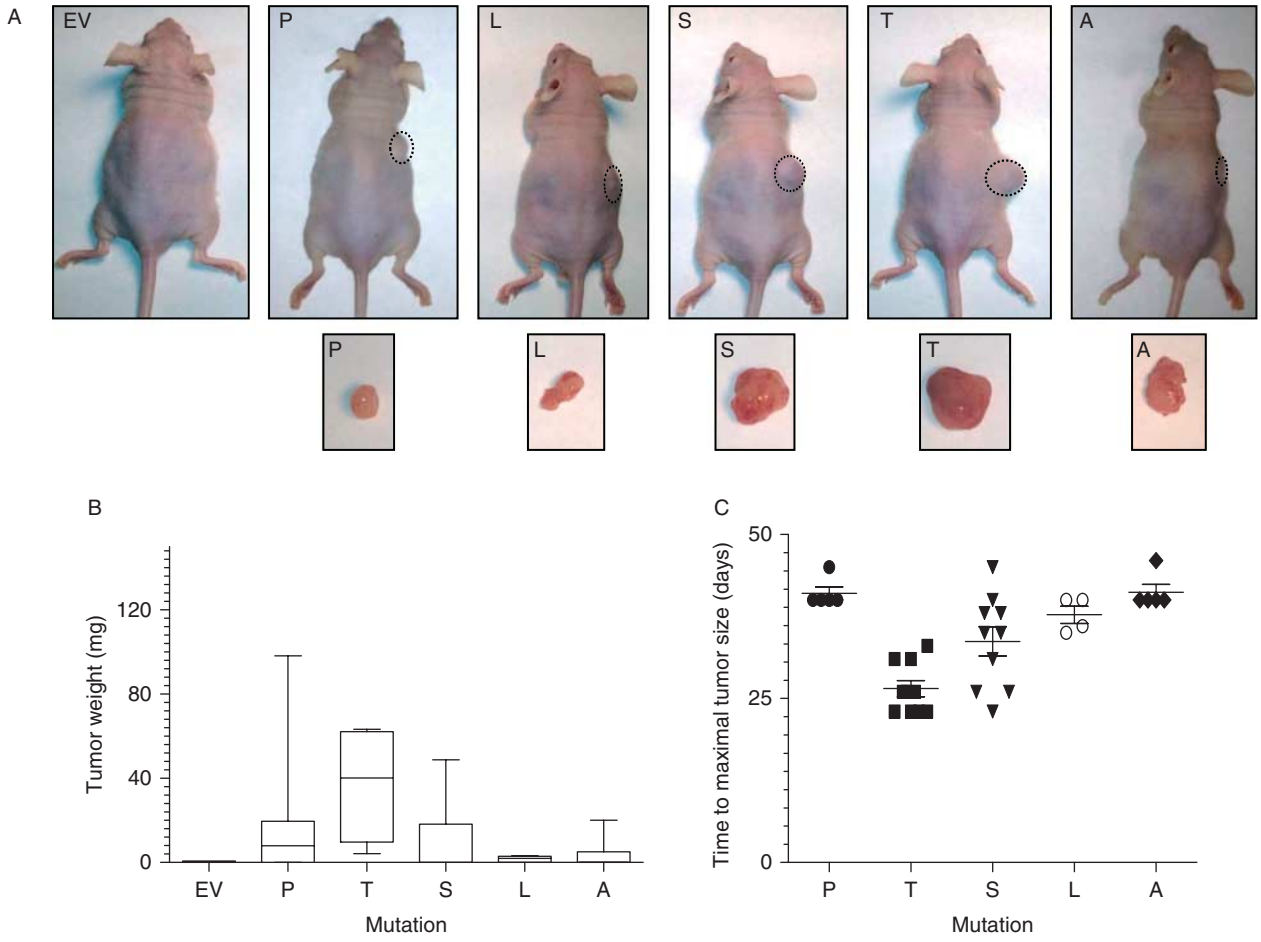

Figure 4

Oncogenic effects of the *HIF2A* mutants *in vivo*. Forty-two nude mice ($n=6$ or 7 per group) were subcutaneously injected with 5×10^6 HEK293 cells stably expressing the indicated constructs (empty vector=EV, Pro531Thr=T, Pro531Leu=L, Pro531Ser=S, and Pro531Ala=A) or a wild-type Pro531 (P) HIF2A construct. Animals were killed after 28 days and tumors were removed. (A) Representative mice and respective tumors are shown. None of the EV-injected mice developed tumors within the observed period. (B) Weight (in mg) of tumors plotted by the type of mutation (EV vs T $P<0.05$ by Kruskal–Wallis). (C) Two additional cohorts ($n=5$–10 mice per group) were used and animals were killed when tumors reached maximum size in accordance with IACUC-approved protocols. Mice that did not develop tumors were excluded from this analysis. Time from injection until maximum size (in days) was plotted (P vs T and *P vs S, $P<0.05$).

supplementary data given at the end of this article) (Kondo *et al*. 2002). Thus, we explored the transforming properties of the 531 mutations with a murine xenograft model. Six to seven nude mice per group were injected subcutaneously with HEK293 cells expressing empty vector, wild-type or mutant *HIF2A* constructs. While mice carrying vector-expressing cells did not form tumors after 28 days, most HIF2A-injected mice developed macroscopic tumors (Fig. 4A). In particular, animals injected with Pro531Thr-expressing cells produced significantly larger tumors than any other cell group (Fig. 4A and B, $P<0.05$). These results were validated in two other cohorts, in which five to ten mice per group developed tumors. In these groups, the tumor latency in mice carrying *HIF2A* Pro531Thr and Pro531Ser-expressing cells was shorter than in those injected with HIF2A without these mutations ($P<0.05$, Fig. 4C). In our model, the remaining mutants, Pro531Leu and the positive control Pro531Ala, did not yield significantly more aggressive tumors (Fig. 4A and B). The mild phenotype of the Pro531Ala-injected cells might suggest a cell type-dependent effect. It is also possible that the transcriptional transactivation properties of the amino acid sequence surrounding the Pro531 region may contribute to mutation-specific differences (Kondo *et al*. 2003, Yan *et al*. 2007). Additional *in vitro* and *in vivo* models may elucidate the reasons for this genotype–phenotype variability.

http://erc.endocrinology-journals.org
DOI: 10.1530/ERC-13-0101

Published by Bioscientifica Ltd.

Discussion

Our data support an oncogenic role for *HIF2A* in cancer and confirm recent reports of somatic mutations of this gene in pheochromocytomas and paragangliomas, which became available as we were completing this study (Burnichon *et al*. 2012, Favier *et al*. 2012, Lorenzo *et al*. 2012, Zhuang *et al*. 2012, Comino-Mendez *et al*. 2013). Furthermore, our work expands on these observations by showing the tumorigenic effect of mutations of the 531 residue *in vivo*. Moreover, our finding of the inhibitory effect of these mutations on chromaffin marker expression suggest that activated HIF2α may contribute to a more aggressive phenotype of target cells, similar to poorly oxygenated areas of various cancers (Semenza 2012). Despite its effect on increased transcription of target genes, expression of the Ser71Tyr mutant did not enhance HIF2α protein stability or resistance to VHL degradation, so a potential 'passenger' effect of this mutation cannot be ruled out.

Despite notable recent advances, the genetic basis of most pheochromocytomas, including those with a pseudohypoxic profile, still remains unresolved. Future investigations may uncover other genetic variations that can strengthen the link between the hypoxia pathways and cancer.

Supplementary data

This is linked to the online version of the paper at http://dx.doi.org/10.1530/ERC-13-0101.

Declaration of interest

The authors declare that there is no conflict of interest that could be perceived as prejudicing the impartiality of the research reported.

Funding

This work was supported by a Voelcker Fund Award and a CTSA-IIMS pilot project as part of the NIH-8UL1TR000149 to P L M Dahia; a Voelcker Fund; and NCI-5R01CA138747 to R C T Aguiar. The Flow Cytometry and DNA Nucleic Acid Core are supported by UTHSCSA, NIH-NCI P30-CA54174 to the Cancer Therapy and Research Center (CTRC at UTHSCSA).

Author contribution statement

R A Toledo designed experiments; processed and extracted nucleic acids from tissues and cell lines; validated mutations; and performed quantitative gene expression, statistical analyses, and preliminary exome analysis. Y Qin was responsible for generating most stable cell line pools and clones and for performing cellular and biochemical studies. S Srikantan generated cell lines and performed biochemical analyses. N P Morales assisted with sample processing and sequencing and generated mutagenized clones. Q Li and S-W Kim performed the mouse xenograft studies, Y Deng assisted with tumor and cell line expression analysis. M A A Pereira provided clinical information. S P A Toledo provided clinical samples and reviewed patients' records. X Su performed bioinformatic and somatic analysis of exomes. R C T Aguiar provided reagents, designed and performed experiments, managed xenograft studies, and analyzed the data. P L M Dahia conceived the study, designed and performed experiments, analyzed the data, and wrote the manuscript, with input from R A Toledo, R C T Aguiar, and other authors.

Acknowledgements

This work is dedicated to the memory of Alberto Antônio Dahia. The authors thank the International Familial Consortium members for their continuing collaboration and the patients and their families for their participation.

References

Acker T, Diez-Juan A, Aragones J, Tjwa M, Brusselmans K, Moons L, Fukumura D, Moreno-Murciano MP, Herbert JM, Burger A *et al*. 2005 Genetic evidence for a tumor suppressor role of HIF-2α. *Cancer Cell* **8** 131–141. (doi:10.1016/j.ccr.2005.07.003)

Burnichon N, Vescovo L, Amar L, Libe R, de Reynies A, Venisse A, Jouanno E, Laurendeau I, Parfait B, Bertherat J *et al*. 2011 Integrative genomic analysis reveals somatic mutations in pheochromocytoma and paraganglioma. *Human Molecular Genetics* **20** 3974–3985. (doi:10.1093/hmg/ddr324)

Burnichon N, Cascon A, Schiavi F, Morales NP, Comino-Mendez I, Abermil N, Inglada-Perez L, de Cubas AA, Amar L, Barontini M *et al*. 2012 MAX mutations cause hereditary and sporadic pheochromocytoma and paraganglioma. *Clinical Cancer Research* **18** 2828–2837. (doi:10.1158/1078-0432.CCR-12-0160)

Comino-Mendez I, de Cubas AA, Bernal C, Alvarez-Escola C, Sanchez-Malo C, Ramirez-Tortosa CL, Pedrinaci S, Rapizzi E, Ercolino T, Bernini G *et al*. 2013 Tumoral EPAS1 (HIF2A) mutations explain sporadic pheochromocytoma and paraganglioma in the absence of erythrocytosis. *Human Molecular Genetics*. (doi:10.1093/hmg/ddt069)

Dahia PL, Ross KN, Wright ME, Hayashida CY, Santagata S, Barontini M, Kung AL, Sanso G, Powers JF, Tischler AS *et al*. 2005 A HIF1α regulatory loop links hypoxia and mitochondrial signals in pheochromocytomas. *PLoS Genetics* **1** 72–80. (doi:10.1371/journal.pgen.0010008)

Favier J, Buffet A & Gimenez-Roqueplo AP 2012 HIF2A mutations in paraganglioma with polycythemia. *New England Journal of Medicine* **367** 2161 (author reply 2161–2162). (doi:10.1056/NEJMc1211953)

Gimenez-Roqueplo AP, Favier J, Rustin P, Mourad JJ, Plouin PF, Corvol P, Rotig A & Jeunemaitre X 2001 The R22X mutation of the SDHD gene in hereditary paraganglioma abolishes the enzymatic activity of complex II in the mitochondrial respiratory chain and activates the hypoxia pathway. *American Journal of Human Genetics* **69** 1186–1197. (doi:10.1086/324413)

Gordan JD, Bertout JA, Hu CJ, Diehl JA & Simon MC 2007 HIF-2α promotes hypoxic cell proliferation by enhancing c-myc transcriptional activity. *Cancer Cell* **11** 335–347. (doi:10.1016/j.ccr.2007.02.006)

Gui Y, Guo G, Huang Y, Hu X, Tang A, Gao S, Wu R, Chen C, Li X, Zhou L *et al*. 2011 Frequent mutations of chromatin remodeling genes in transitional cell carcinoma of the bladder. *Nature Genetics* **43** 875–878. (doi:10.1038/ng.907)

Hillier LW, Marth GT, Quinlan AR, Dooling D, Fewell G, Barnett D, Fox P, Glasscock JI, Hickenbotham M, Huang W *et al*. 2008 Whole-genome sequencing and variant discovery in *C. elegans*. *Nature Methods* **5** 183–188. (doi:10.1038/nmeth.1179)

Jafri M & Maher ER 2012 The genetics of phaeochromocytoma: using clinical features to guide genetic testing. *European Journal of Endocrinology* **166** 151–158. (doi:10.1530/EJE-11-0497)

Published by Bioscientifica Ltd.

Kaelin WG, Jr & Ratcliffe PJ 2008 Oxygen sensing by metazoans: the central role of the HIF hydroxylase pathway. *Molecular Cell* **30** 393–402. (doi:10.1016/j.molcel.2008.04.009)

Kondo K, Klco J, Nakamura E, Lechpammer M & Kaelin WG, Jr 2002 Inhibition of HIF is necessary for tumor suppression by the von Hippel–Lindau protein. *Cancer Cell* **1** 237–246. (doi:10.1016/S1535-6108(02)00043-0)

Kondo K, Kim WY, Lechpammer M & Kaelin WG, Jr 2003 Inhibition of HIF2α is sufficient to suppress pVHL-defective tumor growth. *PLoS Biology* **1** E83. (doi:10.1371/journal.pbio.0000083)

Lee S, Nakamura E, Yang H, Wei W, Linggi MS, Sajan MP, Farese RV, Freeman RS, Carter BD, Kaelin WG, Jr *et al.* 2005 Neuronal apoptosis linked to EglN3 prolyl hydroxylase and familial pheochromocytoma genes: developmental culling and cancer. *Cancer Cell* **8** 155–167. (doi:10.1016/j.ccr.2005.06.015)

Lorenzo FR, Yang C, Ng Tang Fui M, Vankayalapati H, Zhuang Z, Huynh T, Grossmann M, Pacak K & Prchal JT 2012 A novel EPAS1/HIF2A germline mutation in a congenital polycythemia with paraganglioma. *Journal of Molecular Medicine* **91** 507–512. (doi:10.1007/s00109-012-0967-z)

Marth GT, Korf I, Yandell MD, Yeh RT, Gu Z, Zakeri H, Stitziel NO, Hillier L, Kwok PY & Gish WR 1999 A general approach to single-nucleotide polymorphism discovery. *Nature Genetics* **23** 452–456. (doi:10.1038/70570)

Mazumdar J, Hickey MM, Pant DK, Durham AC, Sweet-Cordero A, Vachani A, Jacks T, Chodosh LA, Kissil JL, Simon MC *et al.* 2010 HIF-2α deletion promotes Kras-driven lung tumor development. *PNAS* **107** 14182–14187. (doi:10.1073/pnas.1001296107)

Min JH, Yang H, Ivan M, Gertler F, Kaelin WG, Jr & Pavletich NP 2002 Structure of an HIF-1α–pVHL complex: hydroxyproline recognition in signaling. *Science* **296** 1886–1889. (doi:10.1126/science.1073440)

Pacak K, Jochmanova I, Prodanov T, Yang C, Merino M, Fojo T, Prchal JT, Tischler AS, Lechan RM & Zhuang Z 2013 A new syndrome of paraganglioma and somatostatinoma associated with polycythemia. *Journal of Clinical Oncology*.

Percy MJ, Zhao Q, Flores A, Harrison C, Lappin TR, Maxwell PH, McMullin MF & Lee FS 2006 A family with erythrocytosis establishes a role for prolyl hydroxylase domain protein 2 in oxygen homeostasis. *PNAS* **103** 654–659. (doi:10.1073/pnas.0508423103)

Pietras A, Hansford LM, Johnsson AS, Bridges E, Sjolund J, Gisselsson D, Rehn M, Beckman S, Noguera R, Navarro S *et al.* 2009 HIF-2α maintains an undifferentiated state in neural crest-like human neuroblastoma tumor-initiating cells. *PNAS* **106** 16805–16810. (doi:10.1073/pnas.0904606106)

Qin Y, Yao L, King EE, Buddavarapu K, Lenci RE, Chocron ES, Lechleiter JD, Sass M, Aronin N, Schiavi F *et al.* 2010 Germline mutations in TMEM127 confer susceptibility to pheochromocytoma. *Nature Genetics* **42** 229–233. (doi:10.1038/ng.533)

Qing G & Simon MC 2009 Hypoxia inducible factor-2α: a critical mediator of aggressive tumor phenotypes. *Current Opinion in Genetics & Development* **19** 60–66. (doi:10.1016/j.gde.2008.12.001)

Rai D, Kim SW, McKeller MR, Dahia PL & Aguiar RC 2010 Targeting of SMAD5 links microRNA-155 to the TGF-β pathway and lymphomagenesis. *PNAS* **107** 3111–3116. (doi:10.1073/pnas.0910667107)

Raval RR, Lau KW, Tran MG, Sowter HM, Mandriota SJ, Li JL, Pugh CW, Maxwell PH, Harris AL & Ratcliffe PJ 2005 Contrasting properties of hypoxia-inducible factor 1 (HIF-1) and HIF-2 in von Hippel–Lindau-associated renal cell carcinoma. *Molecular and Cellular Biology* **25** 5675–5686. (doi:10.1128/MCB.25.13.5675-5686.2005)

Selak MA, Armour SM, Mackenzie ED, Boulahbel H, Watson DG, Mansfield KD, Pan Y, Simon MC, Thompson CB & Gottlieb E 2005 Succinate links TCA cycle dysfunction to oncogenesis by inhibiting HIF-α prolyl hydroxylase. *Cancer Cell* **7** 77–85. (doi:10.1016/j.ccr.2004.11.022)

Semenza GL 2012 Hypoxia-inducible factors: mediators of cancer progression and targets for cancer therapy. *Trends in Pharmacological Sciences* **33** 207–214. (doi:10.1016/j.tips.2012.01.005)

Yan Q, Bartz S, Mao M, Li L & Kaelin WG, Jr 2007 The hypoxia-inducible factor 2α N-terminal and C-terminal transactivation domains cooperate to promote renal tumorigenesis *in vivo*. *Molecular and Cellular Biology* **27** 2092–2102. (doi:10.1128/MCB.01514-06)

Zhuang Z, Yang C, Lorenzo F, Merino M, Fojo T, Kebebew E, Popovic V, Stratakis CA, Prchal JT & Pacak K 2012 Somatic HIF2A gain-of-function mutations in paraganglioma with polycythemia. *New England Journal of Medicine* **367** 922–930. (doi:10.1056/NEJMoa1205119)

Received in final form 15 March 2013
Accepted 20 March 2013
Made available online as an Accepted Preprint
26 March 2013

Published by Bioscientifica Ltd.